Intraoperative Tumor Assessment Using Real-Time Molecular Imaging in Head and Neck Cancer Patients

Stan van Keulen, MD, Naoki Nishio, MD, PhD, Shayan Fakurnejad, BSc, Nynke S van den Berg, PhD, Guolan Lu, PhD, Andrew Birkeland, MD, Brock A Martin, MD, Tymour Forouzanfar, MD, PhD, A Dimitrios Colevas, MD, Eben L Rosenthal, MD, FACS

BACKGROUND: In head and neck cancer, surgical resection using primarily visual and tactile feedback is considered the gold standard for solid tumors. Due to high numbers of tumor-involved surgical margins, which are directly correlated to poor clinical outcomes, intraoperative optical imaging trials have rapidly proliferated over the past 5 years. However, few studies report on intraoperative in situ imaging data that could support surgical resection. To demonstrate the clinical application of in situ surgical imaging, we report on the imaging data that are directly (ie in real-time) available to the surgeon.

STUDY DESIGN: Fluorescence intensities and tumor-to-background ratios (TBRs) were determined from the intraoperative imaging data—the view as seen by the surgeon during tumor resection—of 20 patients, and correlated to patient and tumor characteristics including age, sex, tumor site, tumor size, histologic differentiation, and epidermal growth factor receptor (EGFR) expression. Furthermore, different lighting conditions in regard to surgical workflow were evaluated.

RESULTS: Under these circumstances, intraoperative TBRs of the primary tumors averaged 2.2 ± 0.4 (range 1.5 to 2.9). Age, sex, tumor site, and tumor size did not have a significant effect on open-field intraoperative molecular imaging of the primary tumors ($p > 0.05$). In addition, variation in EGFR expression levels or the presence of ambient light did not seem to alter TBRs.

CONCLUSIONS: We present the results of successful in situ intraoperative imaging of primary tumors alongside the optimal conditions with respect to both molecular image acquisition and surgical workflow. This study illuminates the potentials of open-field molecular imaging to assist the surgeon in achieving successful cancer removal. (J Am Coll Surg 2019;229:560–567.

Disclosure Information: Nothing to disclose.

Disclosures outside the scope of this work: Dr Colevas is a member of the Pfizer Data Safety Monitoring Board and is a paid consultant to COTA, Inc, KeyQuest Health, LOXO Oncology, ATARA Biotherapeutics, Aduro Biotech, Inc, Cue Biopharma, Inc, IQVIA RDS, Inc, and PRA Health Sciences. Dr Rosenthal's institution receives equipment loans from Stryker (Novadaq) and LICOR Biosciences.

Support for this study: This work was supported in part by the Stanford Comprehensive Cancer Center, the Stanford University School of Medicine Medical Scholars Program, the Netherlands Organisation for Scientific Research (Rubicon; 019.171LW.022), the National Institutes of Health and the National Cancer Institute (R01CA190306), and the Stanford Molecular Imaging Scholars (SMIS) program (T32CA118681).

Received July 11, 2019; Revised August 14, 2019; Accepted September 3, 2019.

From the Department of Otolaryngology, Division of Head and Neck Surgery (van Keulen, Nishio, Fakurnejad, van den Berg, Lu, Birkeland, Rosenthal), the Department of Clinical Pathology (Martin), and the Department of Medicine, Division of Medical Oncology (Dimitrious Colevas), Stanford University School of Medicine, Stanford, CA, and the Department of Oral and Maxillofacial Surgery/Oral Pathology, VU University Medical Center/Academic Centre for Dentistry Amsterdam (ACTA), Amsterdam, The Netherlands (van Keulen, Forouzanfar).

Correspondence address: Eben L Rosenthal, MD, FACS, Department of Otolaryngology, Stanford University School of Medicine, 900 Blake Wilbur Dr, 94305 Stanford, CA. email: elr@stanford.edu

https://doi.org/10.1016/j.jamcollsurg.2019.09.007
ISSN 1072-7515/19

Abbreviations and Acronyms

EGFR = epidermal growth factor receptor
HNSCC = head and neck squamous cell carcinoma
ROI = regions of interest
SCC = squamous cell carcinoma
TBR = tumor-to-background ratio

For decades, surgeons have almost exclusively relied on visual and tactile cues for surgical tumor resection of head and neck squamous cell carcinoma (HNSCC). Unfortunately, positive surgical margins are found in 20% to 30% of patients at final histopathology 5 to 7 days after the surgery, a percentage that has not changed over the past 30 years.[1-3] This is in part due to the intricate anatomy of the head and neck, with critical unresectable structures and areas of challenging visualization. Subsequently, surgeons often face difficulties in achieving a complete resection without significant loss of function and poor cosmesis.[4-6]

Fluorescence-based intraoperative molecular imaging is a burgeoning field, reflected by the steep rise of clinical trials evaluating novel agents as well as the development of imaging hardware in the near-infrared range to detect these agents.[7,8] Both targeted and nontargeted imaging agents have been shown to be effective for identification of ex vivo tumor specimen and tumor margins with millimeter resolution.[9-11] However, these ex vivo modalities do not provide real-time in situ feedback of the primary tumors within the surgical field.[12] Real-time, tumor-specific molecular imaging could assist the surgeon in intraoperative clinical decision-making. Nonetheless, presenting objective in situ imaging data remains challenging as patient, environmental, and operator variables affect imaging parameters (eg ambient light, camera-to-tissue distance, surgical approach [open vs minimallyinvasive], image post-processing[12,13]), and therefore limit interpatient consistency of intraoperative in situ data. The aim of this study was to evaluate the effect of various patient and tumor characteristics on successful in situ primary tumor visualization and to report on the optimal conditions for image acquisition.

METHODS

Establishment of intraoperative imaging parameters

A phantom experiment was performed to establish the optimal light conditions for the clinical use of real-time intraoperative fluorescence imaging in a standard operating room. An open-field fluorescence imaging device (SPY-PHI, Novadaq) was tested in the operating room under multiple light conditions, using half sphere-shaped tumor tissue-mimicking phantoms loaded with various concentrations of IRDye800CW-carboxylate (excitation/emission max: 774/789 nm; concentrations 0.5 ng/mL, 1.0 ng/mL, 2.0 ng/mL and blank; LICOR Biosciences Inc). Phantom production and composition have been previously described by us and others.[10,14] The effect of the surgical overhead lights (Berchtold, 4,000 k LED, 50/50 Hz, 140W,) and ambient mercury vapor gas lights (16x TL-D, 36W, Philips) on imaging acquisition was tested in the following light settings: both on; overhead light off, ambient on; overhead light on, ambient off; and both off. The fluorescence signal was assessed from the grey-scale imaging data acquired by the fluorescence camera as mean signal intensity (MSI) in arbitrary units (a.u.) using ImageJ (version 1.50i, National Institute of Health). Oversaturation was perceived as phantoms being visually indistinguishable from the next concentration in combination with reaching the maximal grey value of an 8-bit image (ie 255 a.u.) in ImageJ.

Intraoperative primary head and neck squamous cell carcinoma tumor imaging

Twenty patients with biopsy-proven HNSCC, scheduled to undergo surgical resection with curative intent, were included in our ongoing phase I study evaluating the anti-epidermal growth factor receptor (EGFR) antibody panitumumab conjugated to a near infrared dye (panitumumab-IRDye800CW). The study protocol was approved by the Stanford University Institutional Review Board (IRB 35064) and the FDA (NCT02415881), and written informed consent was obtained from all patients. The study was performed in accordance with the Declaration of Helsinki, FDA's ICH-GCP guidelines, and United States Common Rule.

Included patients received an intravenous infusion of 25 mg (n = 4) or 50 mg (n = 18) panitumumab-IRDye800CW (excitation/emission max: 774/789 nm) before surgery, as reported previously.[15] Primary tumors were imaged in the operation room before the first incision was made using the hand-held imaging device (SPY-PHI, Novadaq) optimized for the detection of IRDye800CW. During intraoperative image acquisition, 3 types of imaging modes were evaluated: bright field, fluorescence imaging in grey-scale mode, and fluorescence imaging in a pseudo-colored, heat-map overlay. Throughout image acquisition, camera settings were kept consistent and the overhead lights were turned off to avoid oversaturation of the camera. All imaging data

(ie 8-bit video and still-frame images) gathered during surgery were stored for study purposes.

Imaging analysis of the acquired fluorescence imaging data

After surgery, the fluorescence signal coming from the primary tumor on the stored imaging data was analyzed using ImageJ by calculating tumor-to-background ratios (TBRs) on representive fluorescence grey-scale 8-bit images. The TBRs were calculated by dividing the signal of the area of interest—the primary tumor—to that of background; buccal mucosa in the oral lesions, and gross tumor-negative skin for cutaneous lesions.[15,16] The mean fluorescence signal of the primary tumor was extracted by averaging 10 measurements of circular regions of interest (ROIs) over the gross tumor. The surgeon delineated the tumor area by visual inspection and palpation. The same strategy was performed for the background, where ROIs were selected 30 to 40 mm from the edge of the gross primary tumor. Each tumor and background ROI had exactly the same size of 5 mm in diameter (1,020 pixels per ROI, 1,920 × 1,080 pixel images). Histopathologic evaluation was used to confirm diagnosis and for the concordance of fluorescence signal and tumor tissue of in situ imaging, as previously described.[17] The TBRs were then correlated to different patient and tumor characteristics: sex, age (<60, >60 years), tumor site (lateral tongue, retromolar trigone, other), pathologic tumor T-stage (T1—T2 vs T3—T4) to indicate tumor size, histologic differentiation (well, moderate, and poor), and presence or absence of squamous cell carcinoma (SCC). Assessment of both tumor T-staging and histologic differentiation was performed by a board-certified pathologist.

Epidermal growth factor receptor immunohistochemistry and expression

To assess the EGFR expression in all primary tumors and compare this with intraoperative imaging, the specimens were formalin-fixed overnight, serial sectioned into 5-mm macrosections, and paraffin embedded. Later, a representative 5-μm section was cut from the macrosections. The slides were baked at 60 C° for 1 hour and stained using an autostainer (DAKO Link48 and PT link, Agilent Technologies Inc). Slides were digitized at 20× magnification using a high-resolution slide scanner (NanoZoomer 2.0-RS, Hamamatsu Photonics). The EGFR membrane intensity was scored from 0 to 3+ using a previously established immunohistochemistry staining intensity method.[18,19] The membrane expression score was as follows: 0 if tumor cells had no staining or less than 10% of faint staining; +1 if more than 10% of tumor cells had faint staining; +2 if tumor cells had moderate focal staining; and +3 when tumor cells had strong diffuse EGFR staining. This system of immunohistochemistry interpretation has been validated by the American Society of Clinical Oncology and the College of American Pathologists.[20]

Statistical analysis

Statistical analysis for TBR comparison was performed using the unpaired Mann-Whitney U-test for dichotomous data and the 1-way ANOVA for categorial data with more than 3 units. Results are reported as means ± standard deviations; p values of 0.05 or less were considered significant.

RESULTS

Clinical study

Twenty patients were included in this study. Patient and tumor characteristics are detailed in Table 1. The average patient age was 64 years (range 48 to 76 years); 18 patients presented with biopsy-proven oral cavity cancer and 2 patients with cutaneous cancer. All tumors were completely surgically excised. Final histopathologic assessment concluded invasive SCC in 18 patients. In 2 patients, the excised tissue specimens were found to be negative for SCC despite preoperative biopsies showing SCC.

Intraoperative imaging workflow

All SCC-positive and SCC-negative cases could successfully be imaged intraoperatively using the hand-held fluorescence imaging device. The imaging data were available, in real-time, to the operating surgeon through an LED-screen interface (Fig. 1). Figure 2 displays still-frames from the surgical view of a lateral tongue tumor in the different acquisition modes. In the operating room, the sterile-draped, hand-held device was used to capture images from the surgical field while switching through the different modes (bright field, fluorescence grey-scale, and fluorescence heat-map overlay). Each mode offered the surgeon distinctive information on the primary tumor and its position within the surgical field. The fluorescence heat-map overlay offered signal intensity-based imaging; high fluorescence signal areas (eg primary tumor) were presented to the viewer as red or orange. Therefore, the fluorescence heat-map provided the surgeon with more semiquantitative information about the fluorescence intensity distribution in comparison with other modes. Switching between the different modes allowed the surgeon to correlate primary tumor extent with its anatomic location. It should be noted that the grey-scale imaging mode was found to be the most sensitive imaging mode

Table 1. Patient and Tumor Characteristics

Age, y	Sex	Tumor site	Pathologic TN-stage	Tumor size, mm
71	M	Lateral tongue	T2N0	22
48	M	Lateral tongue	T3N2c	45
58	F	Retromolar trigone	T3N0	45
65	F	Buccal mucosa	T2N2b	35
70	F	Buccal mucosa	T3N0	42
63	F	Alveolar ridge	T2N0	26
71	F	Lateral tongue	T2N2b	21
71	F	Floor of mouth	T1N1	20
47	F	Retromolar trigone	T4bN3b	63
68	F	Lateral tongue	T3N2b	43
75	M	Lateral tongue	Tx*	NA
69	M	Maxillary sinus	T4aN0	53
76	M	Cutaneous - scalp	Tx*	NA
59	F	Lateral tongue	T4aN2c	52
57	F	Retromolar trigone	T4N2c	83
57	M	Lateral tongue	T4aN3b	90
56	M	Retromolar trigone	T4aN0	44
57	M	Cutaneous − neck	T4N0	60
70	M	Lateral tongue	T4aN3b	68
70	M	Lateral tongue	T3N0	45

*Negative for squamous cell carcinoma on final histopathologic assessment.
F, female; M, male; NA, not applicable.

because the overlay of the fluorescence heat-map over the brightfield image obscured fluorescence intensity. Overhead lights (4,000k LED, 50/50Hz) resulted in significant oversaturation of the images (eFig. 1). In contrast, ambient light from ceiling-mounted mercury vapor gas lamps resulted in only a slightly increased fluorescence intensity compared with absence of ambient light. We found that the optimal setting—that with the least disturbance to clinical workflow and adequate imaging data—was when the surgical overhead lights were switched off and ambient ceiling lights turned on.

Fluorescence imaging analysis

Intraoperative fluorescence imaging results correlated to ex vivo imaging and histology for 4 representative patients are shown in Figure 3. In all tumor-positive patients, the primary tumor was consistently brighter when compared with the surrounding normal tissue, with TBRs ranging from 1.5 to 2.9 (average 2.2 ± 0.4). When examining TBR vs patient characteristics, a significant difference in overall TBRs was found when comparing tumor-negative to tumor-positive patients ($p < 0.05$, $n = 20$). No significant differences were observed in TBRs with regard to age, sex, histologic differentiation, T-stage, and tumor site (Fig. 4). Furthermore, no significant difference was found in TBRs between patients who received a 25-mg flat-dose of panitumumab-IRDye800CW vs a 50-mg flat-dose ($p > 0.05$, $n = 18$).

Interestingly, in the patients in whom there was no SCC on final patholgy, the fluorescence signal at the previous biopsy site was similar to that of adjacent tissue (background), as shown by TBRs ranging from 0.9 to 1.0 (average 0.95 ± 0.5). This indicates that the fluorescence signal of the suspicious areas was the same as that of surrounding tissue and consistent with final pathology, which did not identify SCC in the specimen. One patient had a biopsy-positive scalp lesion (SCC) after previous wide local excision, but no residual tumor on final histopathologic assessment. The other case in which imaging showed no fluorescence signal elevation was a lateral tongue resection of a scar from a previous excisional biopsy of an SCC, with final pathology showing no residual tumor. To evaluate the impact of EGFR expression on in situ imaging, we scored the immunohistochemistry membrane intensity (0, 1+, 2+, and 3+) and compared this with the TBRs. All primary tumors had EGFR expression: 1+ was found in 4 tumors, 2+ in 5 tumors, and 3+ in 9 tumors. The intensity score of EGFR is presented in Figure 5, which illustrates that intraoperative TBRs are consistent regardless of EGFR expression levels.

DISCUSSION

We present the results of in situ intraoperative molecular imaging in 20 patients with head and neck cancer to understand the clinical potential of this technology during surgery. We also identified the optimal conditions for image acquisition with respect to surgical workflow. Tumors could clearly be imaged in situ, and all tumors were consistently and significantly brighter when compared with adjacent healthy tissue (average TBR 2.2 ± 0.4, $p < 0.05$). Importantly, we found that in pathologically negative re-resections, the fluorescence signal was equivalent to adjacent background signal (average TBR 0.95 ± 0.5), which supports the value and predictive capability of this technique during surgery.

We believe that the diagnostic data deriving from intraoperative fluorescent imaging will be used by the surgeon in the context of other relevant information, such as tactile and visual feedback. The fluorescent signal therefore does not definitively "rule-in" or "rule-out" disease; it provides an additional layer of information to inform surgical decision-making. From this perspective, the surgeon would incorporate fluorescence imaging with tactile, visual, and preoperative imaging to distinguish healthy from tumor tissue and realize an adequate surgical margin intraoperatively (Figs 2 and 3). In particular, for advanced tumors, tumors with ill-defined visual margins,

Figure 1. Workflow for in situ fluorescence imaging. (a) Schematic concept of real-time fluorescence imaging of a tongue lesion, courtesy of the authors. (b) Hand-held imaging device which combines fluorescence signal information with vivid white light imaging in real-time. (c) Example of a surgical operation using intraoperative fluorescence imaging to visualize primary tumor extent and tumor margins.

re-resections, and anatomically complex sites (eg retromolar trigone and alveolar ridge), fluorescence data may be beneficial in tumor resection.

We found that differences in tumor site and size did not change imaging contrast (as measured by TBR), which suggests that real-time imaging data provided to the surgeon are consistent sources of information. In addition, if the fluorescence signal extends beyond the tumor borders as perceived by visual and tactile information, the surgeon can adjust the surgical margin accordingly. This in situ assessment of tumor margins could therefore potentially lead to a reduced positive margin rate at final pathology. Furthermore, the TBR was consistent across a range of histologic differentiation and EGFR expression. This is in contrast to ex vivo studies using high dynamic range closed-field systems, in which we and others identified a correlation between target (EGFR) expression and fluorescence intensities.[12,21] Moreover, this indifference

Figure 2. Different imaging modes for fluorescence imaging. Intraoperative imaging of a primary tongue squamous cell carcinoma (white arrow), visualized in various modes: (a) bright field, (b) fluorescence grey-scale, and (c) fluorescence heat-map overlay.

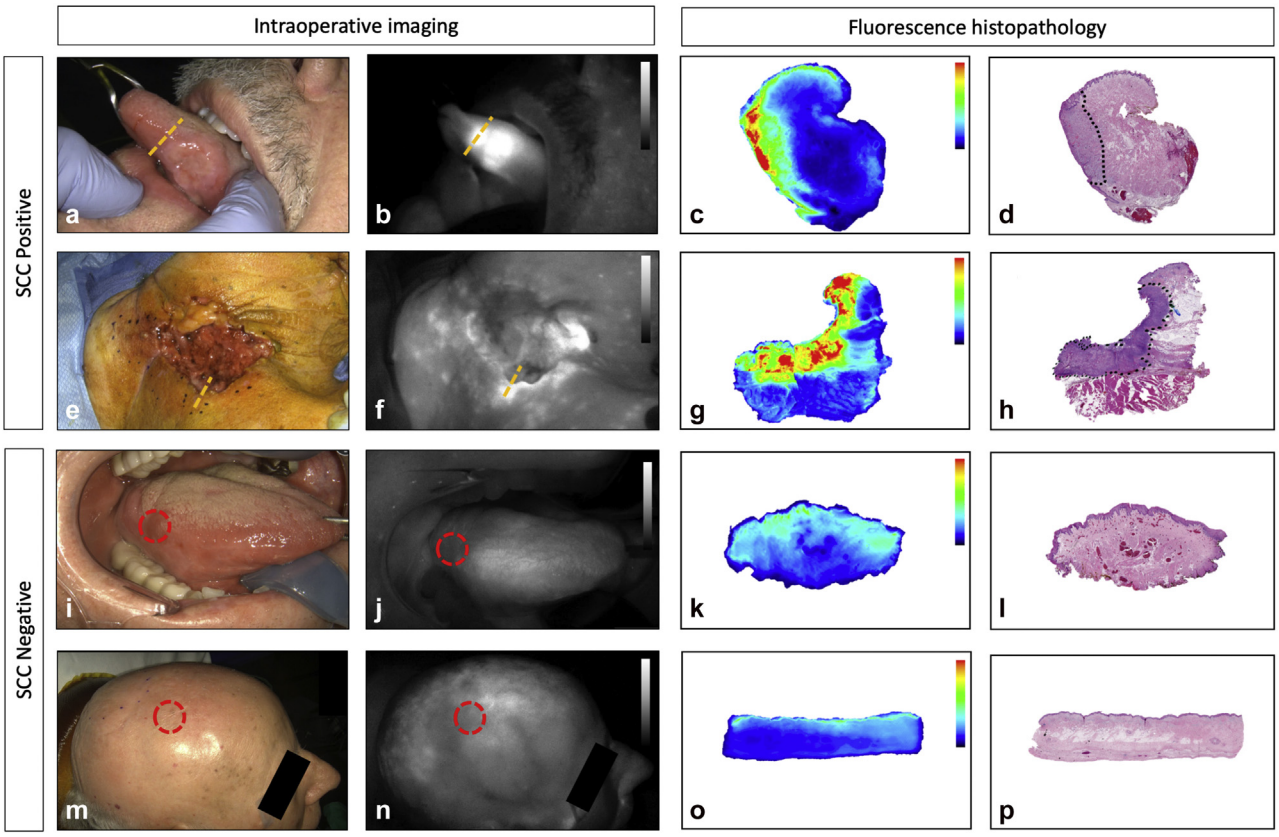

Figure 3. Intraoperative imaging of patients preoperatively determined to have either primary lateral tongue lesion or scalp lesion. Bright field image (a, e, i, and m), in situ imaging (b, f, j, and n), ex vivo imaging (c, g, k, and o) using an Odyssey imaging-platform (LI-COR), and final hematoxylin and eosin (H&E) stained histology (d, h, l, and p). Lesions were assessed for presence of squamous cell carcinoma (SCC); positive (a–h) and negative (i–p) examples are shown. Black dotted line, outlined tumor area; yellow dashed line, fluorescence histopathology location; red circle, location where tumor was thought to be located.

to EGFR expression demonstrated that intraoperative fluorescence imaging is similar between high and low EGFR-expressing tumors.

The main limitation of this study is that imaging results may vary depending on which intraoperative imaging platform is used. Software to accommodate for intensity differences may differ between open-field platforms, creating inconsistency in TBRs when comparing various devices. The purpose of this study, however, was to assess the clinical information that is available to the surgeon using this commercially available imaging device. Furthermore, despite the significant difference that was detected between SCC positive and negative cases, limited conclusions can be drawn from these results due to the small sample size. Also, it should be noted that although this study shows the potential utility of real-time fluorescence imaging for surgical oncology, the true value of this technique will be seen when patient outcomes data, such as prolonged survival, become available.

It is widely recognized that open-field optical imaging is subject to a significant number of external variables such as interference from external light, surface reflectance, and camera placement.[16,22] Yet, it remains difficult to standardize intraoperative data acquisition; the wound cavity depth differs per case, the camera distance to tissue varies per operator and area of interest, the angle of viewing is variable, and ambient light conditions are often different in each operating room.[23] As a result, it is simply not possible to perform rigorous imaging analysis, which controls for these variables. However, because this data set represents the real surgical setting, it ought to be analyzed the way it is interpreted by the surgeon. To this end, we proposed to overcome the absence of true quantitative imaging data by reporting the "surgical view." Furthermore, switching off overhead lights gave a minor interruption of surgical workflow, which can be a burden, especially compared with closed-field ex vivo specimen imaging (image-guided pathology) that does not interfere with

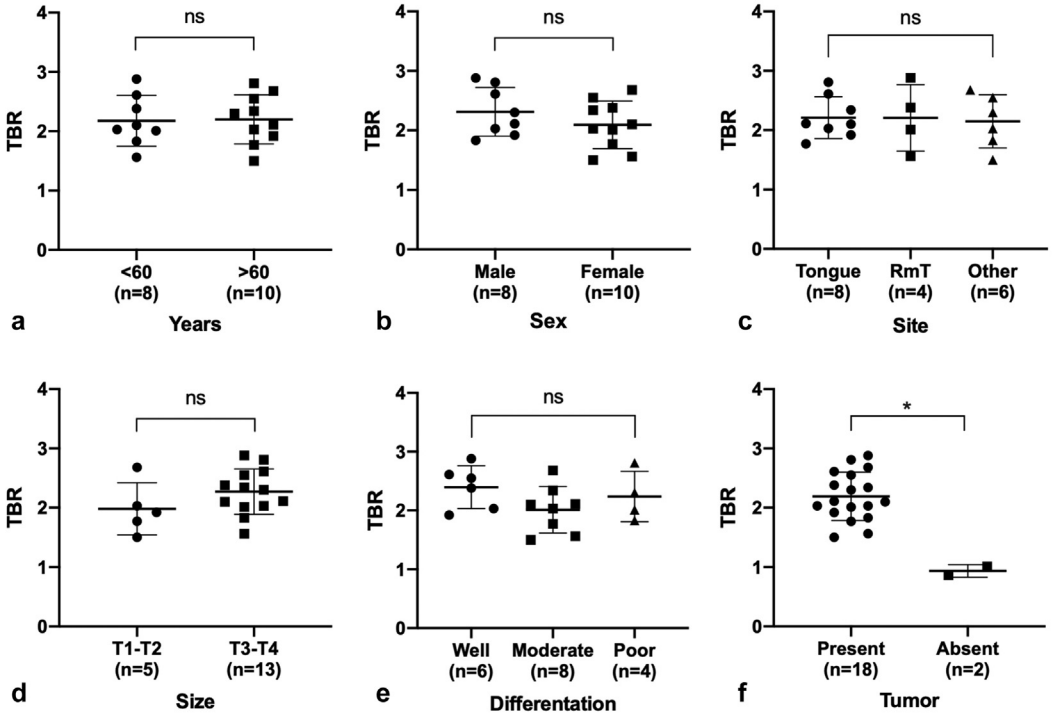

Figure 4. Influence of patient and tumor characteristics on obtained tumor-to-background ratios (TBRs). Tumor fluorescence vs background fluorescence was quantified and TBRs were plotted vs patient (A) age, (B) sex, (C) tumor site, (D) T-stage to indicate tumor size, (E) tumor presence or absence, and (F) histologic differentiation grade. Other, alveolar ridge, buccal mucosa, cutaneaous, floor of mouth, maxillary sinus; RmT, retromolar trigone.

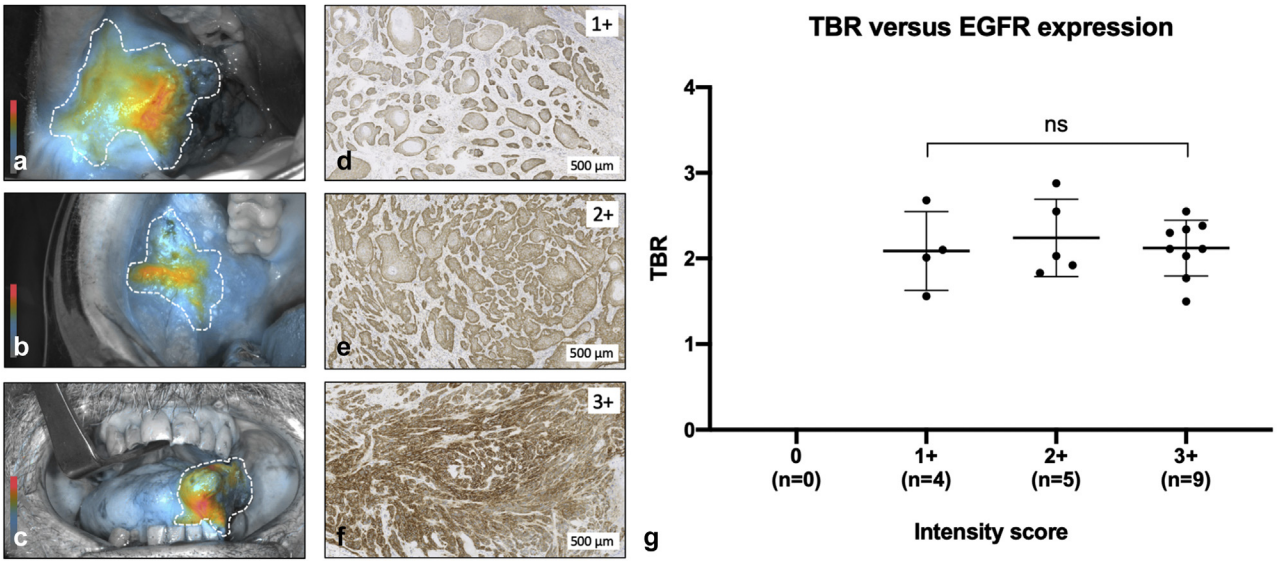

Figure 5. Primary tumor fluorescence tumor-to-background ratio (TBR) vs epidermal growth factor receptor (EGFR) expression. (a-c) In situ tumor visualization in fluorescence heat-map mode. White dashed lines indicate gross primary tumor borders, scale bars indicate intensity range. (d-f) EGFR expression levels (1+, 2+ and 3+), where 0 was left, as this level was not encountered in this study. (g) Graph of TBR vs EGFR expression.

surgical workflow.[24] It is, however, thought that these limitations will become less burdensome as software and hardware continue to evolve collectively. Furthermore, as countless novel near infrared probes are being developed for various cancer types such as lung and breast (eg OTL38, bevacizumab-IRDye800, respectively), we believe that this open-field imaging technique will potentially play a substantial role in surgical oncology in the near future.

CONCLUSIONS

This study demonstrates the potential value of real-time in situ imaging during surgical resection of head and neck tumors. Typically, image analysis in clinical trials is performed in the context of ex vivo imaging, only after resection of the primary tumor has taken place. This study, however, successfully evaluated the surgical view during resection, which is believed to be of great importace during complex intraoperative decision-making.

Author Contributions

Study conception and design: van Keulen, Nishio, Colevas, Rosenthal

Acquisition of data: van Keulen, Nishio, Fakurnejad, van den Berg, Lu, Birkeland, Martin

Analysis and interpretation of data: van Keulen, Nishio, Martin, Rosenthal

Drafting of manuscript: van Keulen, Forouzanfar

Critical revision: Nishio, Fakurnejad, van den Berg, Lu, Birkeland, Forouzanfar, Colevas, Rosenthal

REFERENCES

1. McMahon J, O'Brien CJ, Pathak I, et al. Influence of condition of surgical margins on local recurrence and disease-specific survival in oral and oropharyngeal cancer. Br J Oral Maxillofac Surg 2003;41:224–231.
2. Woolgar JA, Triantafyllou A. A histopathological appraisal of surgical margins in oral and oropharyngeal cancer resection specimens. Oral Oncol 2005;41:1034–1043.
3. Ravasz LA, Slootweg PJ, Hordijk GJ, et al. The status of the resection margin as a prognostic factor in the treatment of head and neck carcinoma. J Craniomaxillofac Surg 1991;19:314–318.
4. Hinni ML, Ferlito A, Brandwein-Gensler MS, et al. Surgical margins in head and neck cancer: a contemporary review. Head Neck 2013;35:1362–1370.
5. Eldeeb H, Macmillan C, Elwell C, Hammod A. The effect of the surgical margins on the outcome of patients with head and neck squamous cell carcinoma: single institution experience. Cancer Biol Med 2012;9:29–33.
6. Pawlik TM, Scoggins CR, Zorzi D, et al. Effect of surgical margin status on survival and site of recurrence after hepatic resection for colorectal metastases. Ann Surg 2005;241:715–722.
7. Chi C, Du Y, Ye J, et al. Intraoperative imaging-guided cancer surgery: from current fluorescence molecular imaging methods to future multi-modality imaging technology. Theranostics 2014;4:1072–1084.
8. Tummers WS, Warram JM, Tipirneni KE, et al. Regulatory aspects of optical methods and exogenous targets for cancer detection. Cancer Res 2017;77:2197–2206.
9. Schaafsma BE, Mieog JSD, Hutteman M, et al. The clinical use of indocyanine green as a near-infrared fluorescent contrast agent for image-guided oncologic surgery. J Surg Oncol 2011;104:323–332.
10. van Keulen S, van den Berg NS, Nishio N, et al. Rapid, non-invasive fluorescence margin assessment: Optical specimen mapping in oral squamous cell carcinoma. Oral Oncol 2019;88:58–65.
11. van Keulen S, Nishio N, Birkeland A, et al. The sentinel margin: intraoperative ex bivo specimen mapping using relative fluorescence intensity. Clin Cancer Res 2019;25:4656–4662.
12. Rosenthal EL, Warram JM, Boer E de, et al. Successful translation of fluorescence navigation during oncologic surgery: a consensus report. J Nucl Med 2016;57:144–150.
13. Keereweer S, Driel PB, Snoeks TJ, et al. Optical image-guided cancer surgery: challenges and limitations. Clin Cancer Res 2013;19:3745–3754.
14. Samkoe KS, Bates BD, Tselepidakis NN, et al. Development and evaluation of a connective tissue phantom model for subsurface visualization of cancers requiring wide local excision. J Biomed Opt 2017;22:1–12.
15. Gao RW, Teraphongphom NT, van den Berg NS, et al. Determination of tumor margins with surgical specimen mapping using near-infrared fluorescence. Cancer Res 2018;78:5144–5154.
16. van Keulen S, Nishio N, Fakurnejad S, et al. The clinical application of fluorescence-guided surgery in head and neck cancer. J Nucl Med 2019;60:758–763.
17. Tummers QR, Verbeek FP, Schaafsma BE, et al. Real-time intraoperative detection of breast cancer using near-infrared fluorescence imaging and methylene blue. Eur J Surg Oncol 2014;40:850–858.
18. Yu J, Kane S, Wu J, et al. Mutation-specific antibodies for the detection of EGFR mutations in non-small-cell lung cancer. Clin Cancer Res 2009;15:3023–3028.
19. Wen YH, Brogi E, Hasanovic A, et al. Immunohistochemical staining with EGFR mutation-specific antibodies: high specificity as a diagnostic marker for lung adenocarcinoma. Mod Pathol 2013;26:1197–1203.
20. Wolff AC, Hammond MEH, Schwartz JN, et al. American Society of Clinical Oncology/College of American Pathologists guideline recommendations for human epidermal growth factor receptor 2 testing in breast cancer. J Clin Oncol 2007;25:118–145.
21. Vorst van der JR, Schaafsma BE, Hutteman M, et al. Near-infrared fluorescence-guided resection of colorectal liver metastases. Cancer 2013;119:3411–3418.
22. Rosenthal EL, Warram JM, Bland KI, Zinn KR. The status of contemporary image-guided modalities in oncologic surgery. Ann Surg 2015;261:46–55.
23. Moore LS, Rosenthal EL, Chung TK, et al. Characterizing the utility and limitations of repurposing an open-field optical imaging device for fluorescence-guided surgery in head and neck cancer patients. J Nucl Med 2017;58:246–251.
24. Teraphongphom N, Kong CS, Warram JM, Rosenthal EL. Specimen mapping in head and neck cancer using fluorescence imaging. Laryngoscope 2017;2:447–452.

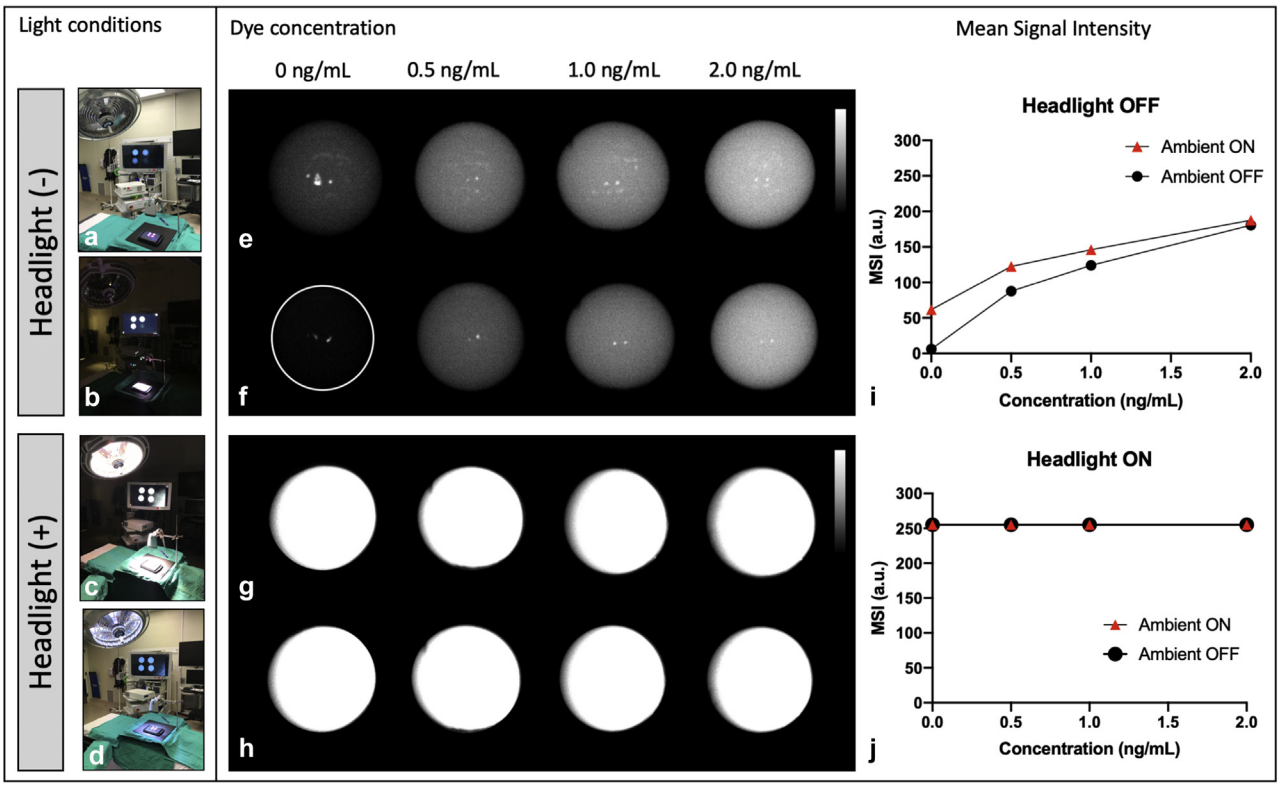

eFigure 1. Identifying optimal light settings for intraoperative in situ fluorescence imaging. Various light settings tested: (a) overhead light off (-), ambient light on (+), (b) all lights off, (c) overhead light on, ambient light off, and (d) all lights on. (e-h) Near-infrared fluorescence imaging of various IRDye800CW loaded phantoms under the light conditions. Visual representation of the phantoms in the fluorescence grey-scale mode. (i-j) Quantification of the visual representation shown in e-h with mean signal intensities of the different dye concentrations showing that in the presence of overhead light camera saturation occurs. au, arbitrary units; MSI, mean signal intensity.